Accepted Manuscript

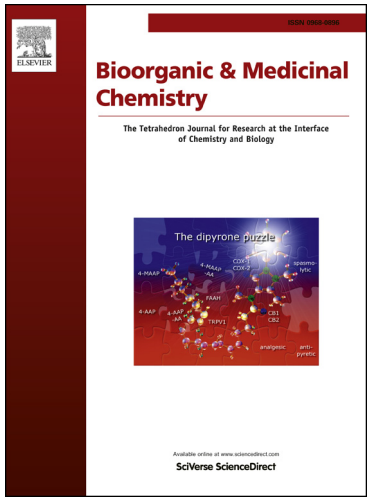

Heterocyclic chlacone activators of nuclear factor (erythroid-derived 2)-like 2 (Nrf2) with improved in vivo efficacy

Nicole Lounsbury, George Mateo, Brielle Jones, Srinivas Papaiahgari, Rajash K. Thimmulappa, Christiana Teijaro, John Gordon, Kenneth Korzekwa, Min Ye, Graham Allaway, Magid Abou-Gharbia, Shyam Biswal, Wayne Childers Jr.

PII: S0968-0896(15)00640-9
DOI: http://dx.doi.org/10.1016/j.bmc.2015.07.056
Reference: BMC 12485

To appear in: *Bioorganic & Medicinal Chemistry*

Received Date: 27 May 2015
Revised Date: 18 July 2015
Accepted Date: 26 July 2015

Please cite this article as: Lounsbury, N., Mateo, G., Jones, B., Papaiahgari, S., Thimmulappa, R.K., Teijaro, C., Gordon, J., Korzekwa, K., Ye, M., Allaway, G., Abou-Gharbia, M., Biswal, S., Childers, W. Jr., Heterocyclic chlacone activators of nuclear factor (erythroid-derived 2)-like 2 (Nrf2) with improved in vivo efficacy, *Bioorganic & Medicinal Chemistry* (2015), doi: http://dx.doi.org/10.1016/j.bmc.2015.07.056

Graphical Abstract

To create your abstract, type over the instructions in the template box below.
Fonts or abstract dimensions should not be changed or altered.

Heterocyclic chalcone activators of nuclear factor (erythroid-derived 2)-like 2 (Nrf2) with improved in vivo efficacy

Leave this area blank for abstract info.

Nicole Lounsbury[a], George Mateo[a], Brielle Jones[b], Srinivas Papaiahgari[b], Rajesh K. Thimmulappa[c], Christiana Teijaro[d], John Gordon[a], Kenneth Korzekwa[a], Min Ye[a], Graham Allaway[b], Magid Abou-Gharbia[a], Shyam Biswal[c*] and Wayne E. Childers, Jr.[a*]

[a]*Moulder Center for Drug Discovery Research, Temple University School of Pharmacy, 3307 N. Broad Street, Philadelphia, PA, USA*
[b]*Cureveda, LLC, 1450 South Rolling Road, Halethorpe, MD 21227, USA*
[c]*Depertmant of Environmental Health Sciences, Johns Hopkins Bloomberg School of Public Health, 615 N. Wolfe Street, Baltimore, MD 21205, USA*
[d]*Department of Chemistry, Temple University, Philadelphia, PA 19122, USA*

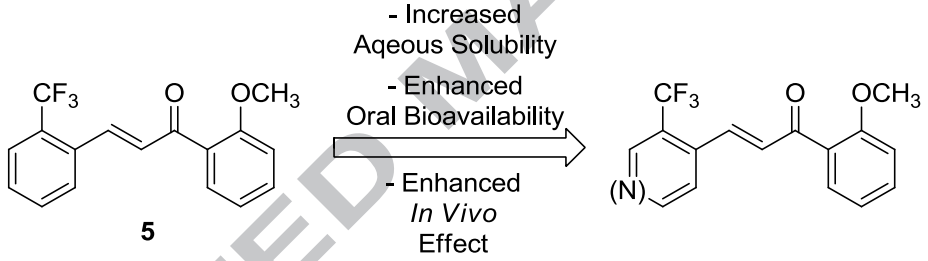

ELSEVIER

Bioorganic & Medicinal Chemistry
journal homepage: www.elsevier.com

Heterocyclic chlacone activators of nuclear factor (erythroid-derived 2)-like 2 (Nrf2) with improved in vivo efficacy

Nicole Lounsbury[a], George Mateo[a], Brielle Jones[b], Srinivas Papaiahgari[b], Rajash K. Thimmulappa[c], Christiana Teijaro[d], John Gordon[a], Kenneth Korzekwa[a], Min Ye[a], Graham Allaway[b], Magid Abou-Gharbia[a], Shyam Biswal[c*] and Wayne Childers, Jr[a*]

[a]*Moulder Center for Drug Discovery Research, Temple University School of Pharmacy, 3307 N. Broad Street, Philadelphia, PA, USA*
[b]*Cureveda, LLC, 1450 South Rolling Road, Halethorpe, MD 21227, USA*
[c]*Depertmant of Environmental Health Sciences, Johns Hopkins Bloomberg School of Public Health, 615 N. Wolfe Street, Baltimore, MD 21205, USA*
[d]*Department of Chemistry, Temple University, Philadelphia, PA 19122, USA*

ARTICLE INFO

Article history:
Received
Received in revised form
Accepted
Available online

Keywords:
Chalcone
Nrf2
Keap1
Bioavailability
Solubility

ABSTRACT

Nrf2 activators represent a good drug target for designing agents to treat diseases associated with oxidative stress. Building upon previous work, we designed and prepared a series of heterocyclic chalcone-based Nrf2 activators with reduced lipophilicity and, in some cases, greater *in vitro* potency compared to the respective carbocylic scaffold. These changes resulted in enhanced oral bioavailability and a superior pharmacodynamic effect *in vivo*.

1. Introduction

Oxidative stress reflects an imbalance between reactive oxygen species (ROS) and reactive nitrogen species (RNS) and a cell's ability to detoxify these reactive species and repair the resulting damage. While some of these reactive species can play a beneficial role (such as in the immune system's response to pathogens), growing evidence implicates oxidative stress in a number of disease states, including cancer, chronic neurodegenerative diseases, cardiovascular disease, diabetes-induced tissue damage and various respiratory diseases such as COPD.[1]

The cell contains a number of defense systems to combat intrinsically and extrinsically induced stressors. For many years, research into oxidative stress focused on superoxide dismutase and the glutathione scavenging system. In 1994,[2] nuclear factor erythroid 2 p45-related factor 2 (Nrf2) was discovered and later shown to be a positive regulator of nearly all cellular antioxidant enzymes through binding to the regulatory element, Antioxidant Response Element (ARE).[3] Nrf2 levels are controlled by binding to the Kelch-like ECH-associated protein 1 (Keap1), a stress (ROS/RNS) sensor that is anchored in the cytoplasm.[4] When bound to Keap1, Nrf2 is ubiquitinated through a Cul3-based E3 ligase pathway and subsequently degraded.[4,5] Exposure to oxidative stress disrupts Keap1-Cul3 ligase activity resulting in stabilization of Nrf2 protein. Higher levels of Nrf2 result in its increased translocation to the nucleus where it binds to the ARE of target genes along with other binding partners, leading to their transcriptional induction.[6-10] The Keap1-Nrf2 system has come to be recognized as a major regulatory pathway of cytoprotective gene expression against oxidative stress and, as such, represents a good drug target for oxidative stress-related diseases.[11,12]

The multiple mechanisms through which Keap1 senses oxidative stress are still not completely understood. However, data from site-directed mutagenesis studies (recently summarized by Suzuki et al.)[12] suggests that one of the sensor mechanisms is a series of cysteine residues that react with ROS/RNS or chemical modifiers to reduce Keap1's ability to target Nrf2 for ubiquitination. In support of this hypothesis, many known Nrf2 activators contain electrophilic groups that are able to react with soft nucleophiles like thiols. Mass spectroscopy and X-ray crystallography have been employed to confirm modification of Keap1 by a number of these compounds.[13] Representative electrophilic Nrf2 activators are shown in Figure 1.[14] Some of these compounds have advanced to clinical trials for various

Corresponding Authors. Tel +1 215 707 1079. Fax +1 215 707 5620 (W. C.); tel +1 410 502 1944. Fax +1 410 955 0116 (S. B.)
Email Addresses: wayne.childers@temple.edu (W. Childers), sbilwal@jhsph.edu (S. Biswal).

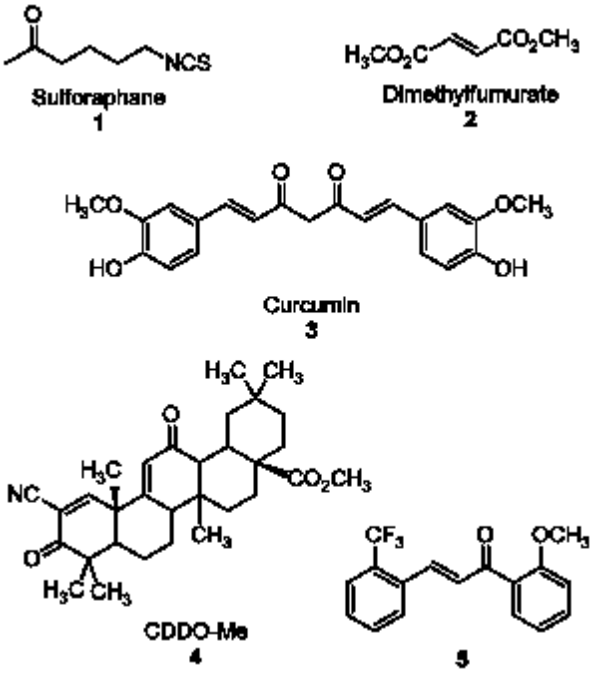

Figure 1. Structures of some known Nrf2 activators.

indications. Among these are sulforaphane (1, the anti-cancer agent discovered in broccoli),[15] CDDO-Me (4, which advanced to clinical trials under the generic name bardoxolone methyl but was terminated in Phase III due to adverse events)[16] and dimethyl fumarate (2), which recently received approval for the treatment of multiple sclerosis under the trade name Tecfidera®.[17]

Some of the authors of the present manuscript recently reported a series of non-cytotoxic chalcone-derived Nrf2 activators, exemplified by compound **5** (Figure 1), that increased the expression of Nrf2-regulated antioxidant genes in human lung epithelial cells and in an *in vivo* mouse model.[18] As a group, chalcones tend to demonstrate low-to-moderate aqueous solubility and modest oral bioavailability due to their lipophilic nature. We sought to enhance the bioavailability of our chalcone series by reducing the lipophilicity through the incorporation of heteroatoms into the aromatic rings. In this manuscript we present the results of that effort.

2. Results and Discussion

2.1 Chemistry.

For the present study, we chose to hold the 2-trifluoromethyl and 2-methoxy groups of **5** constant and introduce pyridine nitrogen atoms into various positions of the two aromatic rings in order to lower lipophilicity. The required heteroaryl chalcones

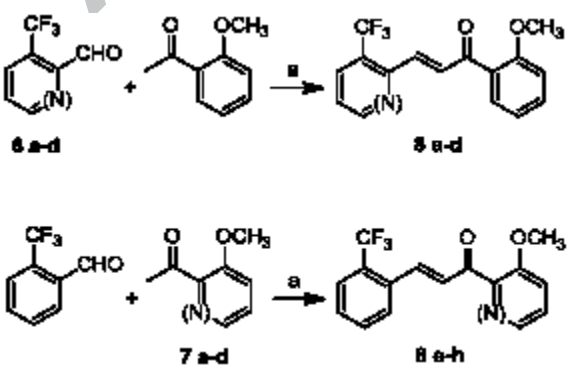

Scheme 1. Synthesis of heteroarylchalcone Nrf2 actovators. Reagents and conditions: (a) LiOH, MeOH, rt, overnight (35 – 83% yield).

were synthesized using the previously described modification of the Claisen-Schmidt reaction (Scheme 1).[18,19] Condensation of (trifluoromethyl)pyridine carboxaldehydes **6a-d** (Table 1) with 2'-methoxyacetophenone in the presence of lithium hydroxide at room temperature overnight gave chalcones **8a-d** (Table 2) in varying yield following purification on silica gel. A similar procedure was used to synthesize chalcones **8e-h** (Table 1) starting with 2-(trifouoromethyl)benzaldehyde and the appropriate methoxy pyridyl-ethanones **7a–d** (Table 1). The final products were obtained as viscous oils that hardened upon standing to give waxy solids. Two of the required intermediates (**6c** and **6d**) were purchased from commercial vendors. Others were not available commercially or their high cost precluded their purchase. We elected to synthesize those intermediates using variations of previously published procedures. The commercially available starting materials and synthetic chemistry references for **6a-d** and **7a-d** are shown in Table 1.

Table 1

Source of Intermediates **6a-d** and **7a-d**

Cd.	Structure	Starting Material	Reference
6a	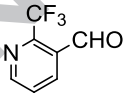	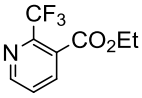	**20**
6b	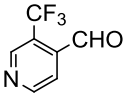	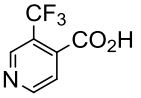	**21**
6c	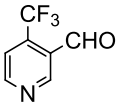	**NA**	**Commercially Available**
6d	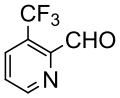	**NA**	**Commercially Available**
7a	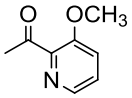	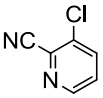	**22**
7b	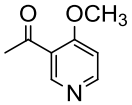	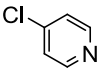	**23**
7c	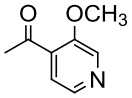	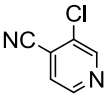	**22**
7d	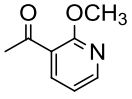	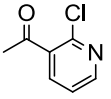	**24**

2.2 Biology.

To examine the ability of the pyridyl chalcones to activat Nrf2, we measured their effect on the expression of the antioxidant gene, heme oxygenase (HO-1), a well-characterized ARE target of Nrf2.[25,26] Normal human bronchial epithelial cells (Beas-2B) were treated with test compounds for 6 hours and HO-1 gene expression levels were determined by quantitative polymerase chain reaction (QPCR) analysis as previously described.[27] Results for the pyridyl chalcones were compared to those obtained for compound **5**. Compound **4**, the known Nrf2

TABLE 2.

Compounds 5 and 8a – 8d. Calculated and Measured Physicochemical Properties.

Compd	Structure	logP	TPSA[a]	Maximum Solubility, uM[b]			Caco-2 P_{app}, 10^{-6} cm/sec[f]	
				PB[c]	SIF[d]	SGF[e]	A - B	B - A
5	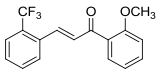	4.61	26.3	13.5	12.8	11.1	17.4	14.6
8a	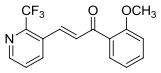	3.78	39.2	50.8	49.8	52.3	nd[g]	nd
8b	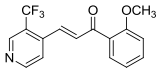	3.39	39.2	172	166	197	nd	nd
8c	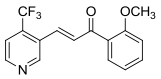	3.39	39.2	134	157	176	nd	nd
8d	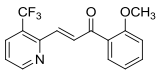	3.63	39.2	90.8	98.6	137	17.3	15.0
8e	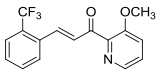	3.78	39.2	170	172	174	nd	nd
8f	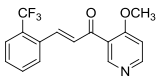	3.39	39.2	23.6	22.5	184	nd	nd
8g	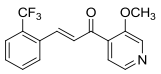	3.39	39.2	53.8	48.2	184	nd	nd
8h	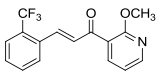	3.99	39.2	40.5	33.6	34.6	nd	nd

[a]Topological polar surface area; [b]Maximum kinetic solubility; [c]Phosphate buffer, pH 7.4; [d]Simulated intestinal fluid; [e]Simulated gastric fluid; [f]Permeability coefficient, bi-directional permeability in Caco-2 monolayers. [g]nd = not determined.

activator clinical candidate CDDO-Me, was included as a positive control and comparator at a concentration of 10 uM. Data are presented in Figure 2.

At a concentration of 5 uM, five of the eight pyridyl chalcone analogs were more effective at activating the expression of HO-1 in Beas-2B cells than the known Nrf2 activator **4** (Figure 2 and Table 3). Three of the five active pyridyl chalcones (**8b**, **8c** and **8g**) were essentially equipotent with the previously reported chalcone **5**, while two of the five active pyridyl chalcones (**8d** and **8f**) were superior to **5**. In particular, compound **8d** enhanced HO1 expression at a concentration of 5 uM, nearly 3-fold higher than the non-heterocyclic chalcone **5**.

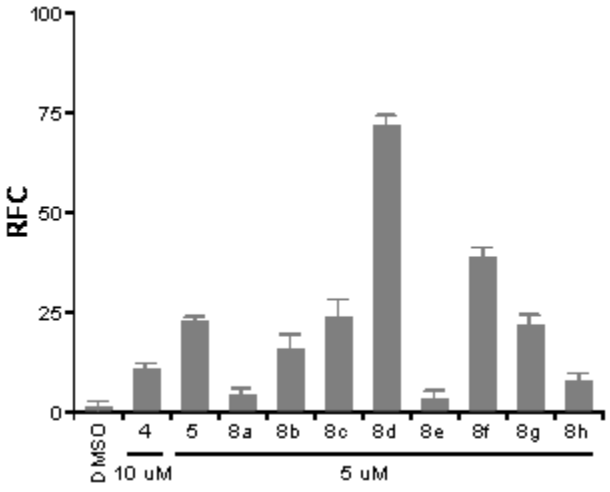

Figure 2. Activation of HO-1 expression in BEAS2-2B cells.

Several factors were considered while trying to understand the structure-activity and structure-property relationships of this series. In general, the pyridyl chalcones were more soluble in aqueous media than the carboxylic analog **5** (Table 2). However, since the cellular assay was run at a concentration of 5 uM, which is less than the maximum aqueous solubility of both **5** and **8a-h**, it is unlikely that solubility limitations played a significant role in the potency differences seen in the Beas-2B assay. Likewise, crystal packing properties were not a contributing factor since all of the test drugs were first dissolved in DMSO prior to use. Compounds **8a-h** displayed somewhat lower logP values compared to **5**, which could have resulted in different permeability properties. But the data from a bi-directional Caco-2 assay suggested that this lower lipophilicity had little effect on permeability (at least for one comparison), and there was no correlation between HO1 levels and logP for the chalcones tested (Table 2). Beas-2B cells can be stimulated to express the efflux transporter p-glycoprotein, although basal expression levels are low.[28] However, literature precedence indicates that chalcones which do interact with p-glycoprotein usually act as inhibitors rather than substrates,[29-31] and the lack of efflux seen in the Caco-2 assay (Table 2) suggests that efflux transport is not playing a significant role in the differences in biological data seen for compounds **5** and **8a-h**.

Another factor that could influence the potency of these chalcones is the reactivity of the electrophilic enone moiety. The lower the LUMO energy, the easier it is for nucleophiles such as thiols to share electrons with the enone, thereby resulting in chemical reaction. This type of analysis is most accurate when

the LUMO energies are calculated using the conformation of the enone-containing molecule that is attacked by the thiol on Keap1, that is, the binding conformation. Since the binding conformation, if any, of these molecules with Keap1 is not known, we used the global minimum energy of each chalcone for our analysis. The results are presented in Table 3.

The calculated LUMO energy of the global minimum energy conformation of **5** was -23.43 kcal/mole. The LUMO energies of the global minimum energy conformations of some of the pyridyl chalcones were indeed lower than that of compound **5**. In particular, the calculated LUMO for the potent analog **8d** was

-28.03 kcal/mol. However, there was not a clear correlation between the differences in activity shown in Figure 2 and the differences in LUMO energy. For example, the calculated LUMO of the global minimum energy conformation of **8b** was

Table 3.

LUMO energies of the global minimum energy conformations of compounds **5** and **8a-h**.

Compound	LUMO (kcal/mol)	Compound	LUMO (kcal/mol)
5	-23.42		
8a	-26.14	**8e**	-21.04
8b	-30.09	**8f**	-23.19
8c	-27.08	**8g**	-24.07
8d	-28.03	**8h**	-22.44

-30.09 kcal/mol yet the compound was less potent than compound **5** in the HO1 expression assay. It is likely that while, overall, LUMO energies for the enone moiety may be playing a role in the greater activity for at least some of the pyridyl chalcones, other factors such as binding interactions with Keap1 may also be contributing to the differences in potency.

We then compared the *in vivo* plasma exposure of the carbocyclic chalcone **5** and the pyridyl chalcone **8d**. The study was supported with *in vitro* data from mouse liver microsomal assays and plasma protein binding assays. Both compounds were given iv at 2 mg/kg and doses orally via gavage at doses of 50, 200 and 400 mg/kg. Plasma levels were quantified by LC/MS/MS at various time points. The results are summarized in Figure 3 and Table 4 (iv data are provided in the supplementary data).

Both **5** and **8d** were metabolized rapidly in mouse liver microsomes, with clearance values > 690 uL/min/mg. However, it appears that both compounds were more stable *in vivo* than predicted by the microsomal stability data, likely due to the high protein binding. Overall, **8d** demonstrated a higher AUC at all three doses than did **5**, resulting in higher bioavailabilities. Based on the Caco-2 data (Table 1), permeability and transporter-mediated efflux do not play an appreciable role in the difference in bioavailability seen between **5** and **8d**. Half-lives for the two compounds following iv administration were similar (**5** – 1.31 hr; **8d** – 1.25 hr. See supplementary data). Accurate half-lives could not be obtained but from Figure 3 it appears that the half-live for compound 8d is somewhat higher than that seen with compound 5, at least at the higher doses. The exposure for both compounds appear to be linear across the doses tested. One likely contributing factor to the enhanced bioavailability seen with **8d** is its improved aqueous solubility compared to **5** (Table 2). Solubility and dissolution rate are well known to have a significant impact on drug absorption.[32] Another likely contributing factor is the longer half-life at the higher doses.

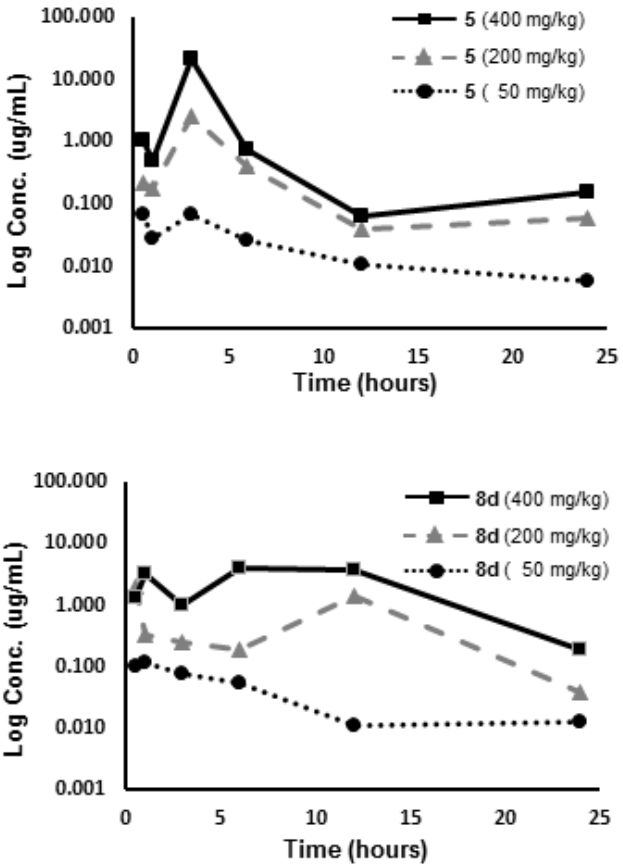

Figure 3. Plasma exposure of **5** and **8d** at 50, 200 and 400 mg/kg po. N = 3 animals per time point. (iv data provided in supplementary data)

Table 4.

Pharmacokinetic properties for **5** and **8d**.

Cd.	AUC[a] (ug/mL•hr)	%F[b]	Microsomal Clint[c] (ul/min/mg)	Stability[c] t1/2 minutes	Protein Binding[e] (% free)
5			> 690	< 2	0.1 %
2 mg/kg[f]	0.38				
50 mg/kg[g]	0.47	5%			
200 mg/kg[g]	7.75	20%			
400 mg/kg[g]	42.7	56%			
8d			> 690	< 2	3.8 %
2 mg/kg[f]	0.302				
50 mg/kg[g]	0.77	10%			
200 mg/kg[g]	11.49	38%			
400 mg/kg[g]	50.4	83%			

[a]Area under the curve; [b]Bioavailability, based on AUC; [c]Mouse liver microsomes; [d]Clint – Free intrinsic clearance [e]Plasma protein binding, % free, unbound fraction; [f]administered i.v.; [g]administered p.o.

Pharmacodynamic studies were also performed on mice treated orally with either 200 mg/kg or 400 mg/kg of compounds **5** and **8d**. Lung tissue from drug-treated and vehicle-treated mice was removed and analyzed for HO1 gene expression HO1 protein levels. Results are shown in Figures 4 and 5. Higher levels of HO1 gene expression (Figure 4) and HO1 protein expression (Figure 5) were observed in the lungs of mice 6 hours post-treatment with **8d** compared to untreated mice, indicating Nrf2 activation. A greater effect on both HO1 gene and protein

expression was seen in mice treated with **8d** compared to those treated with equivalent doses of **5**. These data correlate with the higher *in vitro* potency (Figure 2), higher oral bioavailability (Figure 3, Table 4) and greater free, unbound fraction in plasma (Table 4) demonstrated by compound **8d** compared to that seen with compound **5**.

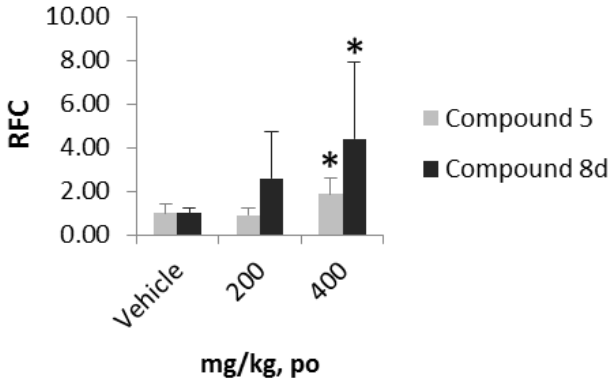

Figure 4. HO1 gene expression in mouse lung relative to vehicle, 6 hours post-treatment (* $P \leq 0.05$).

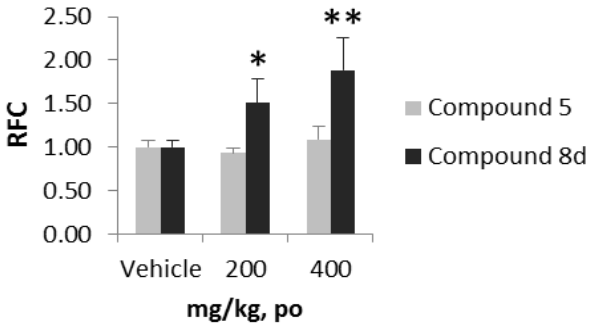

Figure 5. HO1 protein levels in mouse lung relative to vehicle, 6 hours post-treatment (* $P \leq 0.05$; ** $P \leq 0.01$).

3. Conclusion

A series of pyridinyl-chalcones was synthesized and evaluated for the ability to activate HO1, a known ARE target gene for Nrf2. Two of the compounds, **8d** and **8f**, were superior to the clinical candidate **4** and to the previously described carbocyclic chalcone Nrf2 activator **5**. The inclusion of the nitrogen atom into the structure of these new analogs enhanced their aqueous solubility compared to **5**. This increased solubility translated to enhanced oral bioavailability in the case of **8d**, a result that was not influenced by changes in permeability or efflux transport. Lung tissue from mice treated orally with **8d** showed higher levels of both HO1 gene expression and protein expression compared to untreated mice or mice treated with equivalent doses of the carbocyclic chalcone derivative **5**. These results in agreement with the higher *in vitro* potency, greater oral bioavailability and higher free, unbound fraction in plasma seen with 8d and indicate that the compound functions as a Nrf2 activator in vivo.

4. Experimental

4.1 Chemistry

Reagents were purchased from commercial suppliers and used without further purification. Intermediate **6c** was purchased from Frontier Scientific (Logan, UT) and intermediate **6d** was purchased from Combi-Blocks (San Diego, CA). Unless stated otherwise, reactions were run under normal atmospheric conditions. ^{1}H-NMR (400 mHz) and ^{13}C-NMR (100 MHz) data were collected on a Bruker Avance III spectrometer at ambient temperature in the identified solvent. Peak positions are given in parts per million downfield from tetramethylsilane as the internal standard for 1H-NMR spectra. Deuterated chloroform was used as the internal reference for ^{13}C-NMR Normal phase chromatographic separations were performed on silica gel using a Teledyne ISCO Combiflash Rf system. Purity of all final compounds was determined to be ≥95% by reversed phase HPLC on a C-18 column using a gradient of 0–100% acetonitrile in water with 0.1% formic acid as a modifier and UV detection at both 220 nM and 254 nM. High resolution MS was obtained on an Agilent 6520 LC/Q-TOF MS. Compound **5** was synthesized as previously described.[18]

4.1.1 General Method for Producing Pyridyl Chalcones. (*E*)-1-(2-Methoxyphenyl)-3-(2-(trifluoromethyl)pyridine-3-yl)-prop-2-en-1-one (8a).

A solution of lithium hydroxide (0.8 mg, 0.03 mmol)) and 2'-methoxyacetophenone (26 mg, 0.157 mmol) in absolute methanol (1.5 mL) was stirred at room temperature for 15 minutes. To the resulting mixture was added a solution of 2-(trifluoromethyl)-3-pyridinecarboxaldehyde (**6a**, 28 mg, 0.16 mmol) in absolute methanol (15 mL). The reaction was stirred overnight at room temperature (approx. 18 hours). The reaction was then concentrated on a rotary evaporator and the resulting oily residue purified by chromatography on silica gel using a gradient of 0 – 100% ethyl acetate in hexane to provide the desired product (17 mg, 35%) as a light yellow waxy solid. ^{1}H-NMR ($CDCl_3$): δ 8.71 (d, J = 4.9 Hz, 1H), 8.12 (d, J = 8.1 Hz, 1H), 7.93 (dd, J = 15.8 Hz, 2.0 Hz, 1H), 7.68 (dd, J = 7.6, 1.8 Hz, 1H), 7.56 (dd, J = 8.0, 4.6 Hz, 1H), 7.55 (d, J = 7.4 Hz, 1H), 7.54 (dt, J = 7.4 , 1.9 Hz, 1H), 7.36 (d, J = 15,8 Hz, 1H), 7.09 (t, J = 7.6, 1H), 7.03 (d, J = 8.2 Hz, 1H), 3.93 (s, 3H). ^{13}C-NMR ($CDCl_3$) δ 190.8, 157.3, 148.2, 147.1, 145.2, 136.5, 135.1, 134.4, 132.6, 131.6, 129.7, 129.6, 127.2, 125.5, 120.0, 110.6, 54.7. HRMS (FAB): calc'd $C_{16}H_{12}F_3NO_2$ + H = 308.0898, found 308.0889.

4.1.2 (*E*)-1-(2-Methoxyphenyl)-3-(3-(trifluoromethyl)-pyridin-4-yl)prop-2-en-1-one (8b).

Prepared using the general method from lithium hydroxide hydrate (0.6 mg, 0.02 mmol), 2'-methoxyacetophenone (14 mg, 0.112 mmol) and 2-(trifluoromethyl)-4-pyridinecarboxaldehyde (**6b**, 20 mg, 0.114 mmol) in absolute methanol (final reaction volume = 2 mL). The reaction mixture was purified by chromatography on silica gel (gradient of 10 – 100% ethyl acetate in hexane) to give the desired product as a yellow oil (13 mg, 39%). ^{1}H-NMR ($CDCl_3$), δ 8.87 (s, 1H), 8.76 (d, J = 5.2 Hz, 1H), 7.77 (dd, J = 15.8, 2.0 Hz, 1H), 7.62 (dd, J = 7.6, 1.8 Hz, 1H), 7.54 (d, J = 5.2 Hz, 1H), 7.46 (dt, J = 7.6, 1.8 Hz, 1H),7.42 (d, 15.8 Hz, 1H), 7.00 (t, J = 7.6 Hz, 1H), 6.94 (d, J = 8.3 Hz, 1H), 3.85 (s, 3H). ^{13}C-NMR ($CDCl_3$) δ 190.2, 156.9, 156.0, 144.6, 140.9, 140.0, 134.6, 132.2, 129.6, 128.4, 126.3, 126.0, 122.3, 119.0, 113.0, 56.1. HRMS (FAB): calc'd $C_{16}H_{12}F_3NO_2$ + Na = 330.0718, found 330.0719.

4.1.3 (*E*)-1-(2-Methoxyphenyl)-3-(4-(trifluoromethyl)-pyridin-4-yl)prop-2-en-1-one (8c).

Prepared using the general method from lithium hydroxide (3 mg, 0.125 mmol)), 2'-methoxyacetophenone (94 mg, 0.625 mmol)) and 4-trifluoromethyl-3-pyridinecarboxaldehyde (**6c**, 111 mg, 0.635 mmol) in absolute methanol (final reaction volume = 4 mL). The reaction mixture was purified by chromatography on silica gel (gradient of 0 – 100% ethyl acetate in hexane) to give the desired product as a yellow oil (104 mg, 54%). ^{1}H-NMR

($CDCl_3$) δ 8.99 (s, 1H), 8.70 (d, J = 5.5 Hz, 1H), 7.81 (dd, J = 15.8, 2.0 Hz, 1H), 7.63 (dd, J = 7.6, 1.8 Hz, 1H), 7.51 (d, J = 5.5 Hz, 1H), 7.46 (dt, J = 8.4, 1.8 Hz, 1H), 7.42 (d, J = 15.8 Hz, 1H), 7.00 (t, J = 7.6 Hz, 1H), 6.94 (d, J = 8.4 Hz, 1H), 3.94 (s, 3H). ^{13}C-NMR ($CDCl_3$) δ 191.2, 158.5, 151.4, 150.7, 149.4, 136.1, 134.2, 133.9, 132.4, 130.9, 129.1, 128.2, 121.7, 119.5, 111.6, 55.6. HRMS (FAB): calc'd $C_{16}H_{12}F_3NO_2$ + H = 308.0898, found 308.0900.

4.1.4 (*E*)-1-(2-Methoxyphenyl)-3-(3-(trifluoromethyl)-pyridin-2-yl)prop-2-en-1-one (8d).

Prepared using the general method from lithium hydroxide (1.2 mg, 0.01 mmol), 2'-methoxyacetophenone (72 mg, 0.48 mmol) and 3-trifluoromethyl-2-pyridinecarboxaldehyde (**6d**, 85 mg, 0.49 mmol) in absolute methanol (final reaction volume = 4 mL). The reaction mixture was purified by chromatography on silica gel (gradient of 0 – 100% ethyl acetate in hexane) to give the desired product as a yellow oil that hardened upon standing (77 mg, 54%). ^{1}H-NMR ($CDCl_3$) δ 8.82 (d, J = 4.3 Hz 1H), 8.12 (d, J = 15.0 Hz, 1H), 8.01 (dd, J = 8.0, 1.6 Hz, 1H), 7.93 (dd, J = 15.0, 1.9 Hz, 1H), 7.70 (dd, J = 7.6, 1.8 Hz, 1H), 7.51 (t, J = 7.4 Hz, 1H), 7.41 (dd, J = 7.5, 4.6 Hz, 1H), 7.07 (t, J = 7.5 Hz, 1H), 7.02 (d, J = 8.1 Hz, 1H), 3.93 (s, 3H). ^{13}C-NMR ($CDCl_3$) δ 192.4, 158.6, 152.3, 151.6, 135.4, 134.1, 133.9, 133.5, 130.6, 128.8, 125.8, 125.1, 123.2, 120.8, 111.6, 55.7. HRMS (FAB): calc'd $C_{16}H_{12}F_3NO_2$ + H = 308.0898, found 308.0897.

4.1.5 (E)-1-(3-Methoxypyridin-2-yl)-3-(2-(trifluoromethyl)-phenyl)prop-2-en-1-one (8e).

Prepared using the general method from lithium hydroxide (2 mg, 0.05 mmol), 2-(trifluoromethyl)benzaldehyde (47 mg, 0.27 mmol) and 1-(3-methoxypyridin-2-yl)ethanone (**7a**, 40 mg, 0.26 mmol) in absolute methanol (final reaction volume = 6 mL). The reaction mixture was purified by chromatography on silica gel (gradient of o – 100% ethyl acetate in hexane) to give the desired product as yellow oil that hardened upon standing (43 mg, 54%). ^{1}H-NMR ($CDCl_3$) δ 8.33 (dd, J = 4.4, 1.3 Hz, 1H), 8.09 (dd, J = 15.9, 2.1 Hz, 1H), 7.90 (d, J = 7.7 Hz, 1H), 7.73 ((d, J = 7.7 Hz, 1H), 7.71 (d, J = 15.9 Hz, 1H), 7.60 (t, J = 7.6 Hz, 1H), 7.50 (t, J = 7.6 Hz, 1H), 7.47 (dd, J = 8.6, 4.4 Hz, 1H), 7.41 (dd, J = 8.6, 1.3 Hz, 1H), 3.96 (s, 3H). ^{13}C-NMR ($CDCl_3$) δ 190.0, 155.6, 144.3, 140.4, 139.7, 134.1, 132.0, 129.6, 129.3, 129.0, 128.4, 128.1, 127.1, 126.1, 119.8, 55.9. HRMS (FAB): calc'd $C_{16}H_{12}F_3NO_2$ + H = 308.0898, found 308.0899.

4.1.6 (*E*)-1-(4-Methoxypyridin-3-yl)-3-(trifluoromethyl)-phenyl)prop-2-en-1-one (8f).

Prepared using the general method from lithium hydroxide (0.8 mg, 0.032 mmol), 2-(trifluoromethyl)benzaldehyde (28 mg, 0.16 mmol) and 1-(4-methoxypyridin-3-yl)ethanone (**7b**, 24 mg, 0.15 mmol) in absolute methanol (final reaction volume = 1.5 mL). The reaction was purified by chromatography on silica gel (5% methanol in ethyl acetate) to give the desired product as a yellow solid (38 mg, 83%). ^{1}H-NMR ($CDCl_3$) δ 8.64 (d, J = 5.9 Hz, 1H), 7.97 (dd, J = 15.8, 2.0 Hz, 1H), 7.80 (d, J = 7.7 Hz, 1H), 7.75 (d, J = 7.7 Hz, 1H), 7.62 (t, J = 7.5 Hz, 1H), 7.53 (t, J = 7.5 Hz, 1H), 7.35 (d, J = 15.8 Hz, 1H), 6.66 (d, J = 5.9 Hz, 1H), 3.98 (s, 3H). ^{13}C-NMR ($CDCl_3$) δ 190.7, 163.9, 154.0, 151.3, 139.9, 133.8, 132.1, 130.3, 129.8, 128.0, 126.3, 126.2, 125.3, 122.5, 106.9, 55.8. HRMS (FAB): calc'd $C_{16}H_{12}F_3NO_2$ + H = 308.0898, found 308.0899. HRMS (FAB): calc'd $C_{16}H_{12}F_3NO_2$ + H = 308.0898, found 308.0904.

4.1.7 (E)-1-(3-Methoxypyridin-4-yl)-3-(2-(trifluoromethyl)-phenyl)prop-2-en-1-one (8g).

Prepared using the general method from lithium hydroxide (1.75 mg, 0.073 mmol), 2-(trifluoromethyl)benzaldehyde (51 mg. 0.37 mmol) and 1-(3-methoxypyridin-4-yl)ethanone (**7c**, 55 mg. 0.36 mmol) in absolute methanol (final reaction volume = 3 mL). The reaction mixture was purified by chromatography on silica gel (5% methanol in ethyl acetate) to give the desired product as a yellow solid (67 mg, 57%). ^{1}H-NMR ($CDCl_3$) δ 8.50 (s, 1H), 8.40 (d, J = 4.3 Hz, 1H), 7.89 (dd, J = 15.8, 1.9 Hz, 1H), 7.78 (d, J – 7.8 Hz, 1H), 7.72 (d, J = 7.8 Hz, 1H), 7.61 (t, J = 7.5 Hz, 1H), 7.52 (t, J = 7.5 Hz, 1H), 7.40 (d, J = 4.4 Hz, 1H), 7.16 (d, J = 15.8 Hz, 1H), 3.98 (s, 3H). ^{13}C-NMR ($CDCl_3$) δ 191.8, 152.5, 143.0, 140.9, 135.1, 134.6, 133.4, 132.2, 130.0, 129.8, 129.4, 129.1, 126.4, 125.2, 122.6, 55.4. HRMS (FAB): calc'd $C_{16}H_{12}F_3NO_2$ + H = 308.0898, found 308.0899.

4.1.8 (E)-1-(2-Methoxypyridin-3-yl)-3-(2-(trifluoromethyl)-phenyl)prop-2-en-1-one (8h).

Prepared using the general method from lithium hydroxide (1 mg, 0.04 mmol), 2-(trifluoromethyl)benzaldehyde (34 mg, 0.2 mmol) and 1-(2-methoxypyridin-3-yl)ethanone (**7d**, 29 mg, 0.19 mmol) in absolute methanol (final reaction volume = 1.5 mL). The reaction mixture was purified by chromatography on silica gel (40% ethyl acetate in hexane) to give the desired product as a yellow solid (29 mg, 49%). ^{1}H-NMR ($CDCl_3$) δ 8.36 (dd, J = 4.8, 2.0 Hz, 1H), 8.08 (dd, J = 7.4, 2.0 Hz, 1H), 8.05 (dd, J = 15.6, 2.2 Hz, 1H), 7.83 (d, J = 7.8 Hz, 1H), 7.75 (d, J = 7.8 Hz, 1H), 7.63 (t, J = 7.6 Hz, 1H), 7.53 (d, J = 7.5 Hz, 1H), 7.47 (d, J = 15.7 Hz, 1H), 7.05 (dd, J = 7.4, 4.8 Hz, 1H), 4.09 (s, 3H). ^{13}C-NMR ($CDCl_3$) δ 189.3, 160.6, 149.5, 138.9, 137.9, 135.9, 131.0, 130.1, 129.8, 128.6, 126.9, 125.2, 124.5, 121.2, 116.1, 52.8. HRMS (FAB): calc'd $C_{16}H_{12}F_3NO_2$ + H = 308.0898, found 308.0874.

4.2 Calculated logP and TPSA.

Predicted octanol/water partition coefficients (logP) and topological polar surface areas (TPSA) were calculated using the Marvin calculator plugin available in MarvinSketch from ChemAxon (Budapest, Hungary). The logP calculator employs a variation[33] on the atomic fragment method originally described by Viswanadhan et al.[34] The TPSA calculator uses the fragment-based summation method described by Ertl et al.[35]

4.3 Molecular modeling.

Modeling and LUMO energy calculations were performed using the Molecular Operating Environment (MOE),[36] the MMFF94 potential[37] and the MOPAC[38] interface of MOE.

4.4 Solubility assays.

Solubility assays were performed using Millipore MultiScreen®HTS-PFC Filter Plates designed for solubility assays (EMD Millipore, Billerica, MA). The 96-well plates consist of two chambers separated by a filter. Liquid handling was performed using JANUS® Verispan and MTD workstations (Perkin Elmer, Waltham, MA). 4 uL of drug solutions (10 mM in DMSO) are added to 196 uL of the appropriate medium in top chamber to give a final DMSO concentration of 2% and a theoretical drug concentration of 200 uM. Plates are gently shaken for 90 minutes and then subjected to vacuum. Insoluble drug is captured on the filter. 160 uL of the filtrate is transferred to 96-well Griener UV Star® analysis plates (Sigma-Aldrich, St. Louis, MO) containing 40 uL of acetonitrile. The drug concentration in the filtrate is measured by UV absorbance on a Spectromax® Plus microplate reader (Molecular Devices, Sunnyvale, CA) using Softmax Pro software v. 5.4.5. Absorbances at 5 wavelengths (280, 300, 320, 340, and 360 nM) were summed to generate the UV signal. Assays were performed in triplicate. Standard curves were generated by adding 4 uL of 50x of five concentrations of test compounds in DMSO to 40 uL of acetonitrile in UV Star plates followed by 156 uL of the appropriate solubility medium. Analysis and statistics were performed using GraphPad® Prism v. 5.04. Data are reported as

the maximum concentration observed in the filtrate. The following solubility media were used in the assays.

Phosphate buffer (pH 7.4): Millipore-defined universal buffer – 45 mM potassium phosphate, 45 mM sodium acetate, 45 mM ethanolamine, pH = 7.4.
Simulated Intestinal Fluid (SIF): United States Pharmacopeia-defined SIF – 50 mM potassium phosphate, pH 6.8, without pancreatin.
Simulated Gastric Fluid (SGF): United States Pharmacopeia-defined SGF – 0.2% sodium chloride, 84 mM HCl, pH 1.2, without pepsin.

4.4 Caco-2 assay.

Bi-directional permeability was assessed in Caco-2 monolayers.[39] Caco-2 cells (clone C2BBe1) were obtained from American Type Culture Collection (Manassas, VA). Cell monolayers were grown to confluence on collagen-coated microporous, polycarbonate membranes in 12-well plates. The permeability assay buffer was Hanks Balanced Salt Solution containing 10 mM HEPES and 15 mM glucose at a pH of 7.4. The buffer in the receiver chamber also contained 1% bovine serum albumin. The dosing solution concentration was 5 uM for each test compound in the assay buffer. Cell monolayers were dosed on the apical side (A-to-B) or basolateral side (B-to-A) and incubated at 37°C with 5% CO_2. Samples were taken from the donor and receiver chambers at 120 minutes. Each determination was performed in duplicate. The flux of co-doses of Lucifer yellow was also measured for each monolayer to insure the integrity of the monolayer. Samples were assayed by LC/MS/MS. The apparent permeability constant, Papp (x 10^{-6} cm/second), was calculated using established equations.[40]

4.5 Microsomal stability assay.

The clearance of test compounds in mouse liver microsomes was determined at 37°C. Assays were conducted in 96-deep well polypropylene plates. Test compounds (1 uM) were incubated in 0.5 mL of 100 mM potassium phosphate buffer (pH 7.4) with 0.5 mg/mL pooled liver microsomes from male CD-1 mice (Life Technologies, Grand Island, NY), 2 mM tetra-sodium NADPH and 3 mM magnesium chloride for 60 minutes at 37oC with gentle shaking. At five time points, 75 uL of reaction mixture was transferred to 96-shallow well stop plates on ice containing 225 mL of acetonitrile with 0.1 uM propafenone. Control reactions (lacking NADPH) were performed in a similar manner to demonstrate NADPH dependency of compound loss. Standard curves for test compounds were generated using 5 concentrations in duplicate that were processed as above but with zero incubation time. Stop plates were centrifuged at 2,000 xg for 10 minutes and then 170 uL of the supernatants were transferred to a Waters Aquity® UPLC 700 uL 96-well sample plate with cap mat (Waters, Milford, MA). The amount of compound remaining in the supernatant was quantified by LC/MS/MS using a Waters TQ MS (electrospray positive mode) coupled to a Waters Aquity® UPLC (BEH column, C18 1.7 uM, 2.1 x 50 cm, gradient of acetonitrile/water/0.1% formic acid). Propafenone was used as the internal standard. GraphPad® Prism v 5.04 was used for nonlinear fitting of time course data to generate Clint values**.**

4.6 Plasma protein binding.

Equilibrium dialysis was performed as previously described[41] using 96-well equilibrium dialyzer plates with MW cutoff of 5K (Harvard Apparatus, Holliston, MA) and a dual-plate rotator set to maximum speed (Harvard Aparatus, Holliston, MA) located in a 37°C incubator with a 10% CO_2 atmospheric environment. Test compounds (2.5 uM) were added to plasma in DMSO (2 uL, final DMSO concentration 0.4%) to give 10 uM. 200 uL of plasma mixture (pH 7.4) and buffer (Dulbecco's phosphate-buffered saline 1X without calcium and magnesium (Mediatech, Inc., Herndon, VA)) were placed in their respective sides, wells were capped and the plate was then placed in the rotator and allowed to dialyze for 22 hours. Following dialysis, 25 uL of buffer and plasma mixture were removed and mixed with 25 uL of the opposite matrix in 96-well deep plates. Concentrations of analytes from each side of the dialysis plate were determined by LC/MS/MS using a standard curve constructed in the same matrix. The fraction unbound (fu) was calculated by dividing the drug concentration in the buffer side of the dialysis plate by the drug concentration in the plasma side.

4.7 Protocol for quantitative PCR (QPCR). HO1 expression in Beas-2B cells.

The ability of the chalcones to upregulate expression of HO1 was examined in Beas-2B cells using a previously described RT-PCR method.[25] Data are reported as fold-increase in RFC. Normal human bronchial epithelial cells (Beas2B) obtained from the American Type Culture Collection (Manassas, VA) were cultured under recommended conditions. Cells were seeded onto 24-well plates for 16 hours before incubation with test compounds. The cells were treated with indicated concentrations of test compound for 6 hours and total RNA was extracted using a Qiagen RNeasy kit (Qiagen Corporation, Valencia, CA). QPCR of human HO-1 and endogenous control GAPDH was performed by using Assay-on Demand primers and probe sets from Applied Biosystems (Applied Biosystems, Foster City, CA).

4.8 *In Vivo* exposure in mice.

The *in vivo* exposure of compounds **5** and **8d** were measured over a 24 hour period in 6 – 8 week old female C57BL/6 mice (Harlan Labs, Indianapolis, IN; n = 3 animals per time point) following a 2 mg/kg iv dose and doses of 50, 200 and 400 mg/kg dose given orally via gavage. Animals were acclimatized for 72 hours prior to any experimental procedures. They were housed 3-5 per cage on a 12 hour light/12 hour dark cycle and were given free access to food and water. Animals were observed at least once daily for any abnormalities or distress and for the development of infectious disease. Treatment of animals was in accordance with the regulations outlined in the USDA Animal Welfare Act (9 CFR Parts 1, 2 and 3) and the conditions specified in the Guide for the Care and Use of Laboratory Animals (ILAR publication, NEC, 2011, The National Academies Press). Test compounds were administered in a vehicle consisting of 10% Ethanol-90% Sesame Oil/Cremophor EL (55:35). The dosing volume was 0.2 mL/mouse. Animals were observed hourly for signs of distress or poor health. Time points (following drug administration) examined were 0, 30 minutes, 1 hour, 3 hours, 6 hours, 12 hours and 24 hours. Blood was drawn under CO_2 anesthesia by cardiac puncture and collected in tubes containing EDTA. Plasma was isolated by centrifugation at 12,000 rpm for 7 minutes and stored at -20°C until analysis. At the end of the 24 hour study all animals were euthanized by CO_2 inhalation. Drug concentrations in plasma were quantified by LC/MS/MS. Statistics were analyzed using WinNonLin.

4.9 Pharmacodynamic analysis. Effect on HO1 gene and protein expression *in vivo*.

For pharmacodynamics anslysis, mice were dosed orally as described above with 200 or 400 mg/kg of compounds **5** and **8d**, or vehicle alone. Mice were sacrificed 6 hours post-treatment and lungs were excised for gene and protein analysis. Half of the lung's left lobe was homogenized and RNA was extracted using the RNeasy Mini Kit (Qiagen, Valencia, CA). HO1 gene expression was determined by QPCR analysis as described above. The remaining lung tissue was homogenized in o.5 mM

sodium vanadate, 1 mM PMSF in Cell Lysis Buffer (Cell Signaling, Canvers, MA) supplemented with 1 tablet/10mL Complete Mini Protease Inhibitor (Roche, Mannheim, Germany). HO1 protein levels were determined by ImmunoSet HO1 ELISA (Enzo Life Science, Famingdale, NY) and normalized by the total protein in homogenates found using the BCA Protein Assay (Thermo Scientific, Rockford, IL).

Acknowledgements

Caco-2 data were provided by Absorption Systems (Exton, PA). The in-life portion of the in vivo exposure and pharmacodynamics studies and plasma collection were provided by Novel Life Sciences, Inc. (Gaithersburg, MD). This work was funded by Curveda, LLC (Halethorpe, MD).

Supplementary data

Synthetic procedures for producing intermediates **6a**, **6b** and **7a-d**, ^{1}H-NMR and ^{13}C-NMR spectroscopic data for compounds **8a-8h** and PK data following iv administration for compounds **5** and **8d** can be found in the online version at:

References and notes

(1) Hybertson, B. M.; Gao, B.; Bose, S. K.; McCord, J. M. Oxidative stress in health and disease: The therapeutic potential of Nrf2 activation. *Mol. Aspects Med*. **2011**, *32*, 234-246.

(2) Moi, P.; Chan, K.; Asunis, I.; Cao, A.; Kan, Y. W. Isolation of NF-E2-related factor 2 (Nrf2), a Nf-E2-like basic leucine zipper transcriptional activator that binds to the tandem Nf-E2/AP1 repeat of the beta-globulin locus control region. *Proc. Natl. Acad. Sci. USA* **1994**, *91*, 9926-9930.

(3) Venugopal, R.; Jaiswal, A. K. Nrf1 and Nrf2 positively and c-Fos and Fra1 negatively regulate the human antioxidant response element-mediated expression of NAD(P)H:quinone oxidoreductase21 gene. *Proc. Natl. Acad. Sci. USA* **1996**, *93*, 14960-14965.

(4) Itoh, K.; Wakabayashi, N.; Katoh, Y.; Ishii, T.; Igarashi, K.; Engel, J. D.; Yamamoto, M. Keap1 represses nuclear activation of antioxidant responsive elements by Nrf2 through binding to the amino-terminal Neh2 domain. *Genes Dev*. **1999**, *13*, 76-86.

(5) Niture, S. K.; Khatri, R. Jaiswal, A. K. Regulation of Nrf2 – an update. *Free Rad. Biol. and Med*. **2014**, *66*, 36-44.

(6) Kobayashi, A.; Kang, M.-I.; Okawa, H.; Ohtsuji, M.; Zenke, Y.; Chiba, T.; Kazuhiko, I.; Yamamoto, M. Oxidative stress sensor Keap1 functions as an adaptor for Cul1-based E3 ligase to regulate proteasomal degradation of Nrf2. *Mol. Cell. Biol*. **2004**, *24*, 7130-7139.

(7) Sussan, T. E.; Rangasamy, T.; Blake, D. J.; Malhotra, D.; El-Haddad, H.; Bedja, D.; Yates, M. S.; Kombairaju, P.; Yamamoto, M.; Liby, K. T.; Sporn, M. b.; Gabrielson, K. L.; Champoin, H. C.; Tuder, R. M.; Knesler, T. W.; Biswal, S. Targeting Nrf2 with the triterpenoid CDDO-imidazole attenuates cigarette smoke-induced emphysema and cardiac dysfunction in mice. *Proc. Natl. Acad. Sci. USA* **2009**, *106*, 250-255.

(8) Kensler, T. W.; Wakabayashi, N.; Biswal, S. Cell survival responses to environmental stresses via the Keap1-Nrf2-ARE pathway. *Annual Rev. Pharmacol. Toxicol*. **2007**, *47*, 89-116.

(9) Rangasamy, T.; Guo, J.; Mitzner, W. A.; Roman, J.; Singh, A.; Fryer, A. D.; Yamamoto, M.; Kensler, T. W.; Tuder, R.M.; Georas, S. N.; Biswal, S. Disruption of Nrf2 enhances susceptibility to severe airway inflammation and asthma in mice. *J. Exp. Med*. **2005**, *202*, 47-59.

(10) Thimmulappa, R. K.; Mai, K. H.; Srisuma, S.; Kensler, T. W.; Yamamoto, M.; biswal, S. Identification of Nrf2-related genes induced by the chemopreventative agent sulforaphane by oligonucleotide microarray. *Cancer Res*. **2002**, *62*, 5196-5203.

(11) Copple, Ii. M.; the Keap1-Nrf2 cell defense pathway – a promising therapeutic target? *Adv. Pharmacol*. **2012,** *63*, 43-79.

(12) Suzuki, T.; Motohashi, H.; Yamamoto, M. Toward clinical application of the Keap1-Nrf2 pathway. *Trends Pharmacol. Sci* **2013**, *34*, 340-346.

(13) Sekhar, K. R.; Rschakonda, G.; Freeman, M. L. Cysteine-based regulation of the CUL3 adaptor protein Keap1. *Toxicol. Appl. Pharmacol*. **2010**, *244*, 21-26.

(14) Hur, W.; Gray, N. S. Small molecule modulators of antioxidant response pathway. *Curr. Opin. Chem. Biol*. **2011**, *15*, 162-173.

(15) Kensler, T. W.; Egner, P. A.; Agyeman, A. S.; Visvanathan, K.; Groopman, J. D.; Chen, J.-G., Chen, T.-Y., Fahey, J. W.; Talalay, P. Keap1-Nrf2 signaling: A target for cancer prevention by sulphoraphane. *Top. Curr. Chem*. **2013**, *329*, 163-178.

(16) Yates, M. S.; Tauchi, M.; Katsouda, F.; Flanders, K. C.; Liby, K. T.; Honda, T.; Gribble, G. W.; Johnson, D. A.; Johnson, J. A.; Burton, N. C.; Builarte, T. R.; Yamamoto, M.; Sporn, M. B.; Kensler, T. W. Pharmacodynamic characterization of chemopreventative triterpenoids as exceptionally potent inducers of Nrf2-regulated genes. *Mol. Cancer Ther*. **2007**, *6*, 154-162.

(17) Center for Drug Evaluation and Research. New Drug Application # 204063Orig1s000. Clinical Pharmacology and Biopharmaceutics Review. Reference ID: 3123618. US Food and Drug Administration. Rockville, MD. Dated 4/29/2012. Available from: http://www.accessdata.fda.gov/drugsatfda_docs/nda/2013/204063Orig1s000TOC.cfm. Last accessed 09/03/2014.

(18) Kumar, V.; Kumar, S.; Hassan, M.; Wu, H.; Thimmulappa, R. K.; Kumar, A.; Sharma, S. K.; Parmar, V. S.; Biswal, S.; Malhotra, S. V. Novel chalcone derivatives as potent Nrf2 activators in mice and human lung epithelial cells. *J. Med. Chem*. **2011**, *54*, 4147-4159.

(19) Bhagat, S.; Sharma, R.; Sawant, D. M.; Sharma, L.; Chakraborty, A. K. $LiOH{\cdot}H_2O$ as a dual activation catalyst for highly efficient and easy synthesis of 1,3-diaryl-2-propenones by Claisen-Schmidt concensation under mild conditions. J. Mol. Catal. A: Chem. **2006**, *244*, 20-24.

(20) Kao, B.-C.; Doshi, H.; Reyes-Rivera, H.; Titus, D. D.; Yin, M.; Dalton, D. R. 3-Substituted 2-pyridinecarbaldoximes. *J. Heterocyclic Chem*. **1991**, **28**, 1315-1324.

(21) Ashimori, A.; Ono, T.; Uchida, T.; Ohtaki, Y.; Fukaya, C.; Watanabe, M.; Yokoyama, K. Novel 1,4-dihydropyridine calcium antagonists. I.: Synthesis and hypotensive activity of 4-(substituted pyridyl)-1,4-dihydropyridine derivatives. *Chem. Pharm. Bull*. **1990**, *38*, 2446-2458.

(22) LaMattina, J. L. The synthesis of 2-amino-4-(4-imidazolyl)pyridines. *J. Heterocycl. Chem*. **1983**, *20*, 533-538.

(23) Busto, E.; Gotor-Fernandez, V.; Gotor, V. Enantioselective synthesis of 4-(dimethylamino)pyridines through a chemical oxi
dation-enzymatic reduction sequence. Application in asymmetric catalysis. *Adv. Synth. Catal*. **2006**, *348*, 2626-2632.

(24) Trecourt, F.; Marsais, F.; Gungor, T.; Queguiner, G. Improved synthesis of 2,3-disubstituted pyridines by metallation of
2-chloropyridine: A convenient route to fused poly heterocycles. *J. Chem. Soc., Perkin 1* **1990**, 2409-2415.

(25) Chen, X.-L.; Kunsch, C. Induction of cytoprotective genes through Nrf2/antioxidajnt response element pathway: A new therapeutic approach for the treatment of inflammatory diseases. *Curr. Pharm. Design* **2004**, *10*, 879-891.

(26) Alam, J.; Stewart, D.; Touchard, C.; Bonapally, S.; Choi, A. M. K.; Cook, J. L. Nrf2, a cap'n'collar transcription factor, regulates induction of the heme oxygenase-1 gene. *J. Biol. Chem*. **1999**, *274*, 26071-36078.

(27) Kumar, S.; Kingh, B. K.; Prasad, A. K.; Parmer, V. S.; B iswal, S.; Ghosh, B. Ethyl 3',4',5'-trimethoxythionocinnamate modulates NF-dB and Nrf2 transcription factors. *Eur. J. Pharmacol*. **2013**, *700*, 32-41.

(28) Kuzuya, Y.; Adachi, T.; Hara, H.; Anan, A.; Izuhara, K.; Nagai, H. Induction of drug-metabolizing enzymes and transporters iun human bronchial epithelial cells by beclomethasone dipropionate. *IUBMB Life* **2004**, *56*, 355-359.

(29) Bois, F.; Beney, C.; Boumendjel, A.; Mariotte, A.-M.; Conseil, G.; DiPietro, A. Halogenated chalcones with high-affinity binding to p-glycoprotein: potential modulators of multidrug resistance. *J. Med. Chem*. **1998**, *41*, 4161-4164.

(30) Liu, X.-L.; Tee, H.-W.; Go, M.-L. Functionalized chalcones as selective inhibitors of p-glycoprotein and breast cancer resistance protein. *Bioorg. Med. Chem*. **2008**, *16*, 171-180.

(31) Parveen, Z.; Brunhofer, G.; Jabeen, I.; Erker, T.; Chiba, P.; Ecker, G. F. Synthesis, biological evaluation and 3D-QSAR studies of new chalcone derivatives as inhibitors of human p-glycoprotein. *Bioorg. Med. Chem*. **2014**, *22*, 2311-2319.

(32) Amidon, G. L.; Lennernas, H.; Shah, V. P.; Crison, J. R. A theoretical basis for a biopharmaceutic drug classification: the correlation of in vitro drug product dissolution and in vivo bioavailability. *Pharm. Res*. **1995**, *12*, 413-420.

(33) Szegezdi, J.P. Scizmadia, F. Prediction of distribution coefficient using microconstants. Poster presented at the 227th ACS National Meeting, March 28 – April 1, 2004, Anaheim, CA. Available on the world wide web at: http://www.chemaxon.com/conf/Prediction_of_distribution_coefficient_using_microconstants.pdf. Last accessed 09/16/2014.

(34) Viswanadhan, V. N.; Ghose, A. K.; Revankar, G. R.; Robins, R. K. Atomic physicochemical parameters for three dimensional structure directed quantitative structure-activity relationships. 4. Additional parameters for hydrophobic and dispersive interactions and their application for an automated superposition of certain naturally occurring nucleoside antibiotics. *J. Chem Inf. Comput. Sci*. **1989**, *3*, 163-172.

(35) Ertl, P.; Rohde, B.; Selzer, P. Fast calculation of molecular polar surface area as a sum of fragment-based contributions and its application to

the prediction of drug transport properties. *J. Med. Chem*. **2000**, *43*, 3714-3717.

(36) MOE Version 2013.08, Chemical Computing Group (Montreal, CA), available at: http://www.chemcomp.com/MOE-Molecular_Operating_Environment.htm. Last accessed 10/02/2014.

(37) Halgren, T. A. Merck molecular force field. I. basis, form, scope, parameterization and performance of MMFF94. *J. Comput. Chem*. **1996**, *17*, 490-519.

(38) Stewart, J. J. P. Optimization of parameters for semiempirical methods I. method. *J. Comput. Chem*. **1989**, *10*, 209-22.

(39) Hidalgo, I. J.; Raub, T. J.; Borchart, R. T. Characterization of the human colon carcinoma cell line (Caco-2) as a model system for intestinal epithelial permeability. *Gastroenterology* **1989**, *96*, 736-749.

(40) Hubatsch, I.; Ragnarsson, E. G. E.; Artursson, P. Determination of drug permeability and prediction of drug absorption in Caco-2 monolayers. *Nat. Protocols* **2007**, *2*, 2111-2119.

(41) Kochansky, C. J.; McMasters, D. R.; Lu, P.; Koeplinger, K. A.; Kerr, H. H.; Shou, M.; Korzekwa, K. R. Impact of pH on plasma protein binding in equilibrium dialysis. *Mol. Pharm*. **2008**, *5*, 438-448.